Seismic Memory in Stone: Structural and Geological Evidence of Historical Earthquakes at the Acropolis of Athens

D. Egglezos [1], D. Moullou[2], V. Evgenikou[3]

[1]*Phd Civil Engineer, GEO.PER. S.A. & DOMOS S.A. SA, Hellenic Open University, dimitrios.egglezos@gmail.com*

[2]*Dr Archaeologist, Ephorate of Antiquities in East Attica, Hellenic Open University, tmoullou@culture.gr*

[3] *Surveying Engineer MSc, vevge@hotmail.com*

ABSTRACT

This paper develops a forensic reconstruction of historical earthquake demand at the Acropolis using two independent “mechanical archives”: (i) the Acropolis Circuit Wall (CW), a composite gravity retaining system that preserves both localized collapse and sector-specific permanent deformation, and (ii) a joint-controlled limestone block detachment at the Areopagus. The CW response is evaluated using staged, nonlinear pseudostatic Soil–Structure Interaction (SSI) analyses representing the cumulative mechanical history of the wall and its backfills, including construction and modification phases, ageing/degradation, rainfall/pore-pressure episodes, excavation/unloading and re-filling, and a sequence of historical earthquakes. The guiding hypothesis is that the 1705 earthquake must simultaneously explain collapse of the eastern CW sector and permanent deformation/cracking of the southern sector, while the cornice-bearing sector of the north wall is interpreted as having collapsed primarily during the 1805 earthquake.

Seismic demand is expressed as an effective acceleration a_{eff} and related to PGA by a_{eff} ≈ 2/3 PGA the use of a_{eff} for permanent deformation and threshold assessment is supported by dynamic–pseudostatic calibration within the CW study (*GEO.PER. S.A. & DOMOS S.A., 2023*). The Areopagus detachment is back-analysed using Limit Equilibrium (LE) and verified with pseudostatic SSI, yielding a critical acceleration a_{crit} = 0.23 g for initiation of joint sliding. Independently, CW collapse initiation of the eastern benchmark section occurs at a_{EW} = 0.21 g under a displacement-based performance criterion (K1). The small difference between these thresholds is interpreted as a consequence of modelling philosophy: the CW analyses adopt characteristic (conservative) structural parameters appropriate for intervention design, so the derived collapse acceleration is interpreted as a lower-bound estimate rather than a best-estimate threshold.

Instrumental evidence is introduced from the 19-07-2019 NW Attica, M=5, earthquake recorded by four accelerographs on the Acropolis Hill. Three stations indicate EW/NS ratios of approximately 2.0–2.4, implying NS PGA amplitudes around 40–50% of EW PGA for a NW-source event at the site (ITSAK, 2019). One crown-mounted sensor exhibits higher PGA and a lower EW/NS ratio, interpreted as crest-level amplification rather than free-field input. Accordingly, directionality is incorporated through a_{NS} ≈ (0.4 ÷ 0.5) a_{EW} (central value 0.5), strengthening the physical basis for sector-selective outcomes without altering the adopted south and north wall NS inputs used in the staged-history validations. The combined evidence provides a consistent reconstruction of the dominant historical shaking affecting the Acropolis and a transferable workflow for comparable heritage sites.

Keywords: forensic geomechanics; staged history analysis; pseudostatic SSI; gravity retaining wall; rock joint sliding; directionality; historical earthquakes; Acropolis

INTRODUCTION

Long-lived heritage systems preserve earthquake “memory” through collapse, permanent deformation, cracking patterns, displaced architectural elements, and rockfalls. However, such signatures rarely reflect a single event acting on an unchanged system. Construction and repair phases, excavation or backfilling, progressive ageing of blocks and interfaces, and environmental actions (wetting–drying cycles, transient pore pressures) alter boundary conditions and resistance. As a result, forensic interpretation requires a coupled view of the structure and its evolving geotechnical setting.

The Acropolis of Athens provides a suitable testbed because two independent archives of strong shaking coexist: (i) the Circuit Wall (CW), a composite gravity retaining system with sector-dependent damage states (Areas A1-A8, Sections S1-S21; Figure 1), and (ii) a nearby joint-controlled detachment at the Areopagus (Figure 2). This study proposes a structured workflow that constrains historical earthquake demand by combining staged pseudostatic SSI of the CW with an independent joint-sliding threshold reconstruction of the Areopagus detachment, expressed through a common intensity parameter (a_{eff}). The emphasis is placed on the 1705 earthquake as the principal trigger of east-wall collapse and the initiator of the south-wall permanent deformation signature, and on the 1805 earthquake as the decisive event for collapse of the cornice-bearing sector of the north wall (characteristic section: SP1; Fig.1), (Egglezos & Moullou, 2022).

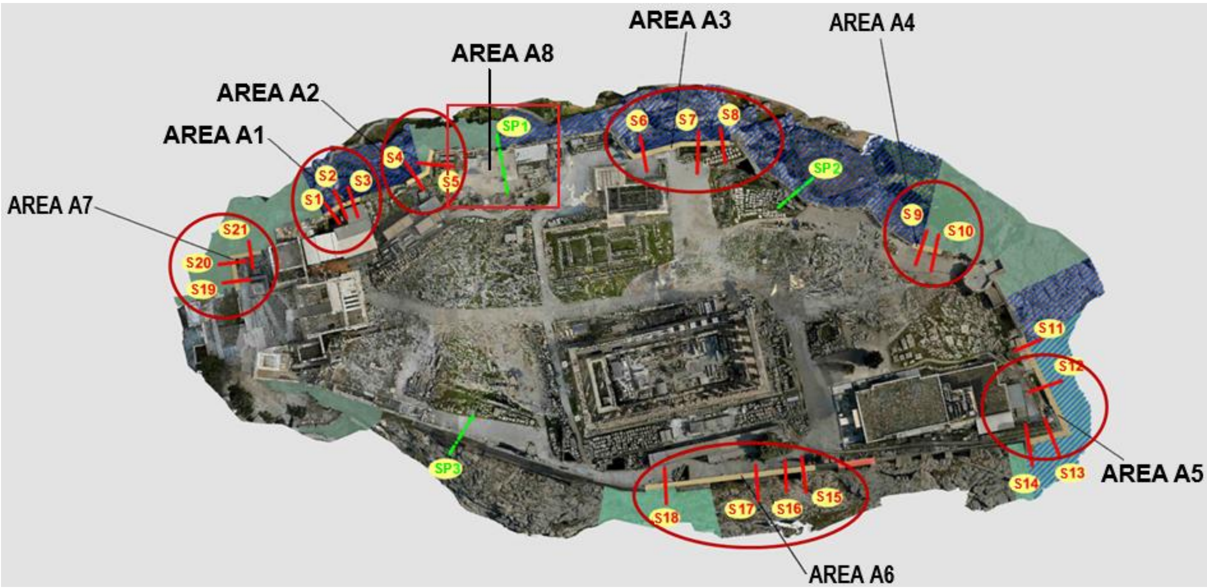

Figure 1. *Landscape of the Acropolis terrace with the 8 areas differing in structural features and damage state (YSMA 2020, GEO.PER. S.A. & DOMOS S.A., 2023).*

Figure 2. *Plan view of the Aeropagus hill which is located near the Acropolis of Athens, along with detached parts of the original rock. Adapted from: Evgenikou, 2017*

OBSERVATIONAL CONSTRAINTS AND GUIDING HYPOTHESIS

Sector-selective CW damage signatures

The reconstruction of te seismic past targets three outcomes:

- Eastern CW sector (S11 – Area A5): collapse attributed to 1705. This sector is treated as the collapse benchmark because the observed failure state indicates a threshold exceedance requiring reconstruction/major intervention (Ambraseys, 1996; Korres, 1996; Papazachos & Papazachou, 2003, Egglezos & Moullou, 2022, Egglezos 2022).
- Southern CW sector (S18 – Area A6): permanent deformation/cracking without collapse dominance. The south sector preserves a cumulative displacement signature consistent with repeated loading and evolving boundary conditions (Ambraseys, 1996; Korres, 1996; Papazachos & Papazachou, 2003, Egglezos & Moullou, 2022, Egglezos 2022).
- Northern CW sector (cornice-bearing area: SP1 - Area A8): collapse attributed primarily to the 1805 earthquake, consistent with the temporal clustering of damage phases and the interpretation of progressive deterioration culminating in collapse (Egglezos & Moullou, 2022).

These observations define the guiding hypothesis:

The 1705 earthquake must simultaneously explain (i) collapse of the eastern CW sector (Figure 3) and (ii) permanent deformation/cracking of the southern CW sector (Figure 4); the north-wall cornice-sector collapse is attributed primarily to the 1805 earthquake (Figure 5).

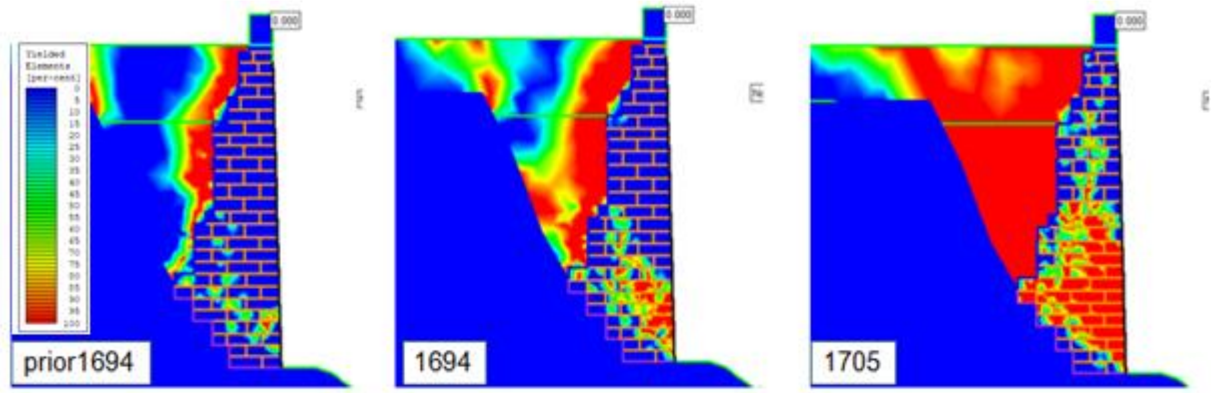

Figure 3. *Development of plastic zones and structural damage in the area near the middle of the eastern sector of CW (Area A5) during the 1694 and 1705 seismic events (Egglezos & Moullou, 2022; Egglezos et al., 2022).Colour scale: red = fully plastic zone; blue = fully elastic zone; intermediate colours indicate transitional stress/plasticity states.*

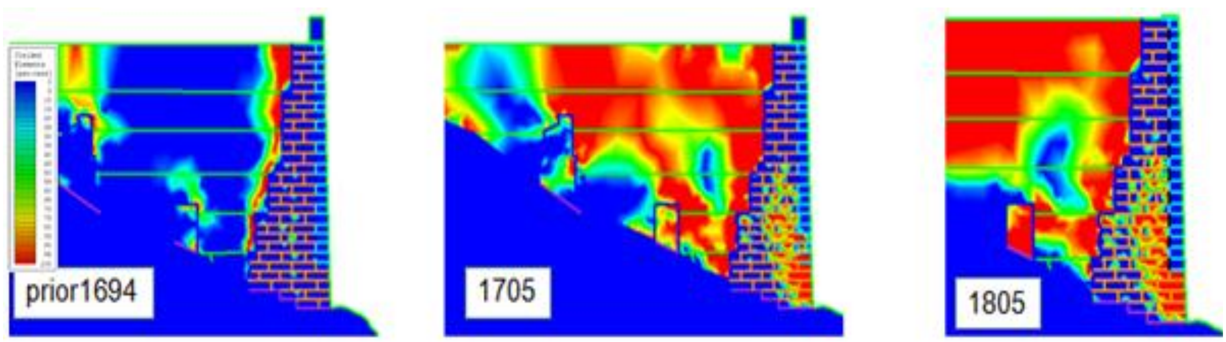

Figure 4. *Development of plastic zones and structural damage on the southern section of the CW in a cross-section near the middle of the Parthenon (Area A6) (after Egglezos & Moullou, 2022; Egglezos et al., 2022). Colour scale: red = fully plastic zone; blue = fully elastic zone; intermediate colours indicate transitional stress/plasticity states.*

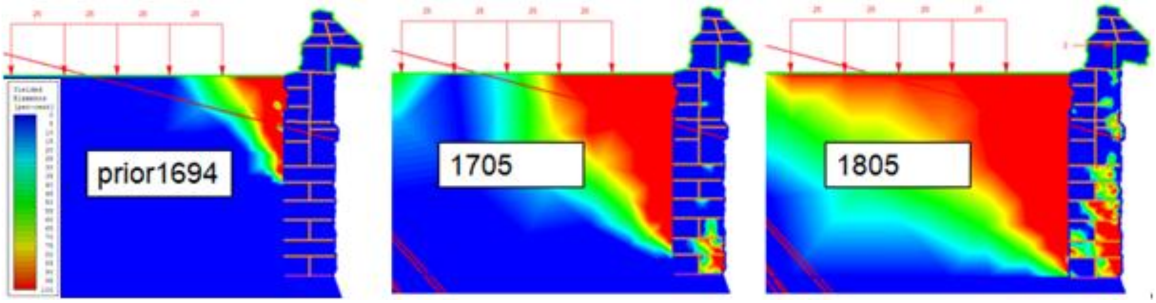

Figure 5. *Plastic zones and structural damage on the northern section of the CW in the area where the cornice are located (Area A2) during the 1705 and 1805 seismic events (after Egglezos & Moullou, 2022; Egglezos et al., 2022). Colour scale: red = fully plastic zone; blue = fully elastic zone; intermediate colours indicate transitional stress/plasticity states.*

Areopagus detachment as an independent mechanical archive

The Areopagus rockfall is interpreted as detachment of a large limestone block along a mapped discontinuity. Because the failure plane is known, a threshold back-analysis is feasible: LE provides the acceleration for FS=1 (initiation), while SSI verification checks that deformation localizes on the same interface and leads to large displacement consistent with detachment. Figure 6, estimates the shape of the “reconstructed” hill.

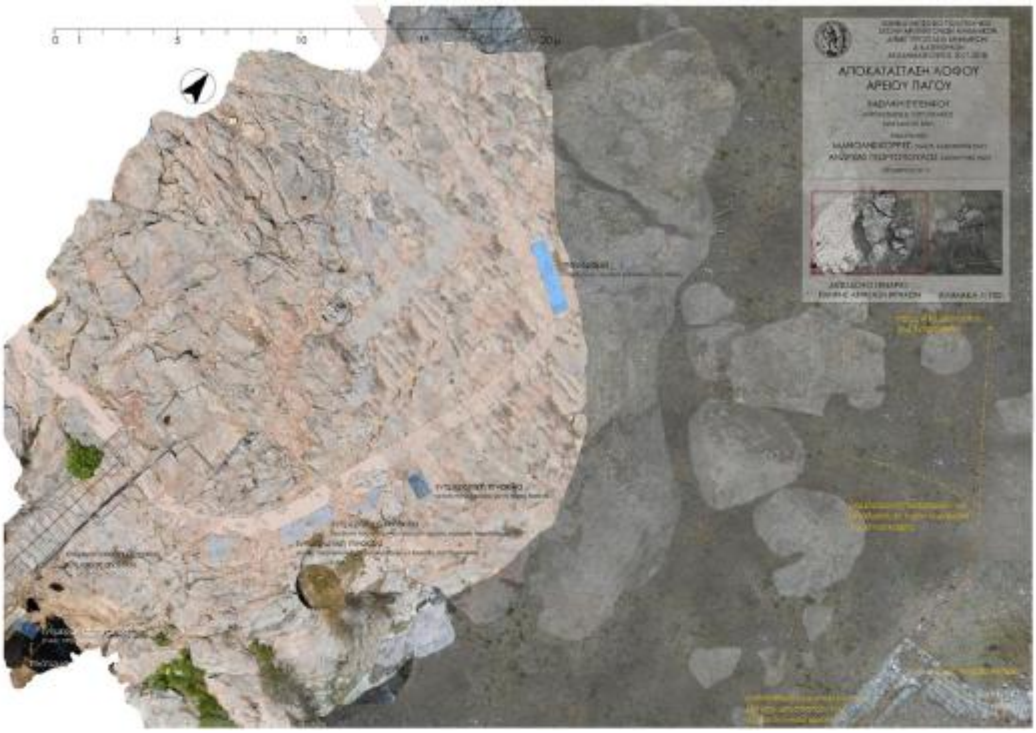

Figure 6. *Areopagus detachment reconstruction (Evgenikou, 2017).*

SEISMIC HISTORY AND SEISMIC INPUT DEFINITION

Late 17th–early 19th century earthquake set (1694–1805)

The staged-history CW analyses emphasize the late 17th–early 19th century, when multiple earthquakes affected the Athens region (Table 1). Within this set, the 1705 and 1805 events are treated as dominant contributors to the CW damage record at the Acropolis, while 1694, 1726 and 1785 are treated as secondary in terms of structural impact for the specific sectors considered (Ambraseys, 1996; Korres, 1996; Papazachos & Papazachou, 2003, Egglezos & Moullou, 2022). This event set is used to define component-dependent effective accelerations for pseudostatic analyses, supporting consistent inputs across sectors and stages.

Table 1. *Seismic events (year, source region, epicentral distance R, Magnitude), estimated PGAs (PGA[1] Skarlatoudis, 2003;) and effective accelerations under different EC8 provisions(Soil category, topography) and standard deviations scenarios*

Event year	Epi-centre [1]	R[1] (km)	M[1]	PGA[2] range (soil A) [min–ave-max] (g)	$a_{eff,EW}$ for east wall (soil A) (g)	$a_{eff,NS}$ for south wall (soil B) (g)	$a_{eff,NS}$ for north wall (soil A) (g)	Observed / interpreted CW effect
1694	Chalkida	47.7	6.2± 0.36	0.045 - 0.066 - 0.096	0.053	0.032	0.026	No specific, widely reported CW damage attribution
1705	North Attica	11.5	6.3	0.229 - 0.332 - 0.485	0.210	0.126	0.105	Collapse of east sector + structural damage; initiates south permanent deformation
1726	Chalkida	59.8	6	0.028 - 0.041 - 0.059	0.039	0.020	0.016	No specific, widely reported CW damage attribution
1785	Chalkida	48.9	6	0.036 - 0.052 - 0.075	0.050	0.025	0.021	Possible contribution to north-wall deterioration (cornice sector)
1805	North of Athens	24.2	6	0.080 - 0.116 - 0.169	0.166	0.083	0.069	Primary collapse trigger for north cornice sector; adds south cumulative displacement

1, Papazachos et al., 2003, 2: std =0, without topographic effect

Effective acceleration and dynamic–pseudostatic calibration

Seismic demand is represented as an effective acceleration a_{eff} appropriate for threshold and permanent deformation assessment:

$$a_{eff} \approx \frac{2}{3} PGA$$

The intended scope of a_{eff} is not to replicate transient time-history response but to represent a demand level that produces comparable permanent deformation and damage-state transitions in calibrated pseudostatic SSI. Dynamic–pseudostatic calibration is used in the CW framework to justify this mapping for the investigated sections and intensity range (Egglezos and Moullou, 2022

Soil category and topographic amplification

Soil class A is adopted for the east wall, the north cornice sector, and the Areopagus area; soil class B is adopted for the south wall/backfilled zones. The CW modelling uses:

$$a_{eff.B} \approx 1.2 \cdot a_{eff,A}$$

as an amplification relationship consistent with the EC8-based differentiation adopted in the CW framework (CEN 2004/2005).

Directionality constrained by site recordings

Directionality is incorporated through a site-supported relationship between components for NW-source shaking:

$$a_{NS} \approx (0.4 - 0.5)a_{EW} \qquad \text{(central value } a_{NS} \approx 0.5 \cdot a_{EW}\text{)}$$

This relationship is used to reconcile sector-selective outcomes: EW-dominant demand controls east collapse, whereas NS demand governs cumulative deformation in the south and contributes to progressive deterioration in the north culminating in collapse in 1805.

Instrumental evidence: 19-07-2019 NW Attica earthquake at the Acropolis

Four accelerographs installed on the Acropolis Hill recorded the 19-07-2019 NW Attica earthquake with a magnitude of M≈5.1–5.3 (Figure 7). Reported PGA values (Table 2) indicate marked component asymmetry at three stations (ACRA, ACRE, ACRJ), with EW/NS ratios approximately 2.44, 2.18, and 1.97, respectively; these correspond to NS PGA amplitudes of about 0.41–0.51 of EW PGA. A fourth sensor (ACRK), located at a specific crown position on the south wall, recorded higher PGA and a lower EW/NS ratio (≈1.41), interpreted as crest-level amplification (and/or local structural contribution) at the instrumented point rather than a representative free-field input proxy. Accordingly, directionality for NW-source shaking at the site is inferred primarily from the mutually consistent set (ACRA, ACRE, ACRJ), while ACRK is treated as an amplification indicator relevant to local response interpretation and dynamic calibration.

Table 2. *Maximum accelerations documented from different accelerometers for the seismic event of Parnetha at 19-07-2019 with magnitude ML=5.1//5.3. Original data from ITSAK.*

Parnetha Seismic Event 19-07-2019: M=5.1/5.3			
Accelerometer	**Max Acceleration (cm/s^2) Direction**		**Ratio R(EW/NS)**
	EW	**NS**	
ACRA	106,88	43,74	2,44
ACRE	111,19	51,1	2,18
ACRK*	*251,03*	*177,78*	*1,41*
ACRJ	85,17	43,17	1,97

*Spectrum Acceleration?

Figure 7. Acropolis array Accelerograph Locations

METHODOLOGICAL APPROACH

Circuit Wall: staged nonlinear pseudostatic SSI

Representative CW sections are analysed using staged nonlinear SSI to represent the evolving mechanical state of the wall–backfill–foundation system. The staged sequence includes construction/modification phases, backfill parameter phases (representing changes in compaction/state), interface ageing/degradation, rainfall/pore-pressure episodes, excavation/unloading and re-filling, and sequential application of historical earthquakes. Two validation tracks are emphasized:

- South wall (S18): staged history from 1694 to 1999 is used to quantify cumulative crest displacement and isolate the contributions of 1705 and 1805 events (Ambraseys, 1996; Korres, 1996; Papazachos & Papazachou, 2003, Egglezos & Moullou, 2022, Egglezos et al., 2022).

- North wall (cornice sector): staged interpretation targets cumulative deterioration culminating in collapse attributed primarily to 1805; 1726 and 1785 are treated as minor contributors relative to 1705 and 1805 for this response (Ambraseys, 1996; Korres, 1996; Papazachos & Papazachou, 2003, Egglezos & Moullou, 2022).

Performance criterion and collapse definition (K1)

CW performance is evaluated using a displacement-based criterion (K1) expressed through the crest displacement normalized by wall height:

$$\frac{\delta_{crest}}{H}$$

In this paper, collapse is defined as K1 threshold crossing (δ/H). This definition is applied consistently to (i) the east-wall collapse benchmark in 1705 and (ii) the north cornice-sector collapse attributed primarily to 1805. The limits of the performance levels are presented in Table 3.

Table 3. *Performance criteria and Damage Levels (D1–D4) used for classification of response in retaining conditions (thresholds for normalised top displacement) (Egglezos & Moullou, 2022; Egglezos, 2022; GEO.PER. S.A. & DOMOS S.A., 2023).*

Normalized (by Height) Relative Roof-to-Base Drift	Performance Level – Limit State
< 2%	D1 – Almost full functionality
2% – 5%	D2 – Limited damage
5% – 10%	D3 – Significant damage
10% – 15%	D4 – Near collapse

Areopagus: LE thresholding with SSI verification

The Areopagus detachment is analysed via LE to determine the effective acceleration that yields FS=1 along the mapped failure plane. SSI verification is then used to check that slip localizes on the same discontinuity at the critical acceleration and that large displacement is produced consistent with detachment. Material properties used in the analyses for the Aeropagus Hill are presented in Table 4.

Table 4. *Areopagus model inputs: rockmass and joint parameters and analysis assumptions*

Parameter	Units	Limestone Rockmass		Schist stone Rockmass		Joints
		Intact Values	Jointed Values	Intact values	Jointed values	
GSI	-	100	55	100	15	-
Compressive Strength	MPa	60	4.8	28	0.14	-
Modulus of Elasticity	GPa	15.6	12.2	0.4	0.3	-
Normal Stiffness	GPa/m	-	-	-	-	60

Shear Stiffness	GPa/m	-	-	-	-	12
c_{peak}	kPa	-	-	-	-	96
φ_{peak}	°	-	-	-	-	59
$c_{residual}$	kPa	-	-	-	-	0
$\varphi_{residual}$	°	-	-	-	-	30

RESULTS

Independent threshold: Areopagus detachment (1705)

The Areopagus back-analysis yields:

- $a_{crit} = 0.23\ g$ for initiation of joint sliding using Limit Equilibrium analyses, which is also verified by pseudostatic SSI (Figure 8).

This value is treated as an independent mechanical benchmark for joint-controlled instability in the local limestone setting.

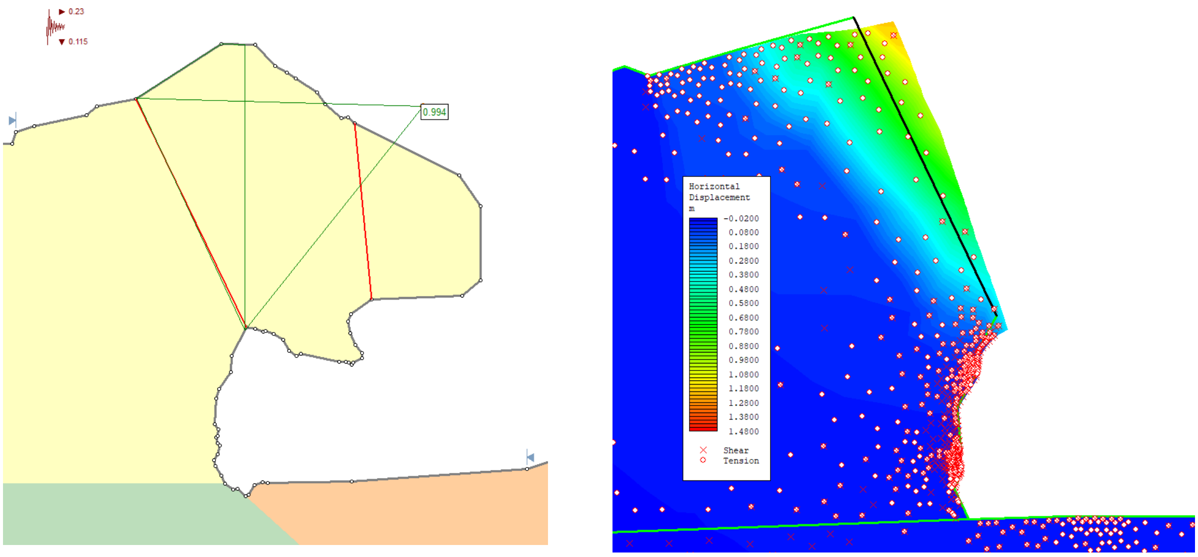

Figure 8. *Result of Limit Equilibrium analysis for the seismic event with $a = a_{crit} = 0.23g$. $FS_{Janbu} = 0.994$ (Left). Results of the SSI analysis. Displacement and yielded elements of Areopagus detachment at $a = a_{crit} = 0.23g$ (Right)*

Eastern CW sector (S11): EW-controlled collapse initiation (1705)

For the eastern collapse benchmark section (Figure 9):

$a_{EW,collapse} = 0.21\ g$, defined by K1 threshold crossing (collapse).

The proximity of $a_{crit} = 0.23\ g$ (Aeropagus) and $a_{EW,collapse} = 0.21$ (east wall) is meaningful because it emerges from independent systems and mechanisms. The observed difference is interpreted as a consequence of modelling philosophy: the CW analyses employ characteristic (conservative) structural properties adopted for intervention design; thus, the wall collapse threshold is interpreted as a lower-bound demand estimate rather than a best-estimate value. The 2019 Acropolis recordings support a directionality relationship in which NS PGA is typically 40–50% of EW PGA for a NW-source event, reinforcing the component-based interpretation used for the sector-selective damage narrative.

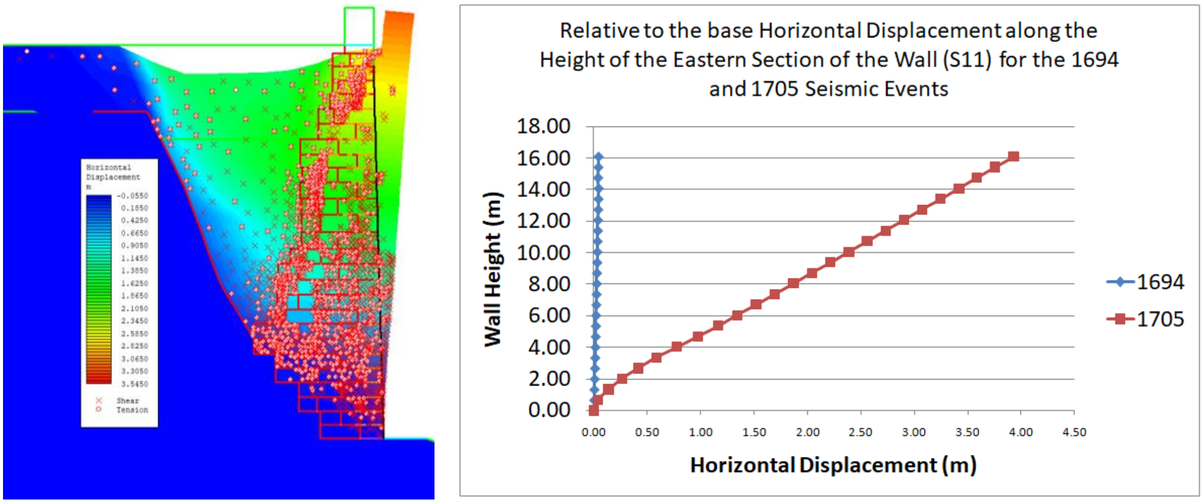

Figure 9. *Horizontal Displacement, yielded elements and areas of the East wall in Area A5 (S11) under seismic load of* $\boldsymbol{a_{EW} = 0.21\,g}$ *(Left). Relative to the base Horizontal Displacement along the height of the wall during the 1694 and the 1705 (=collapse) seismic event (Right).*

Southern CW sector (S18): cumulative permanent deformation (1694–1999 staged history)

The staged-history validation for the south wall uses the NS pathway and yields a cumulative deformation signature dominated by the 1705 and 1805 events with adopted inputs:

- $a_{1705,SW} = 0.13\ g$ (soil class B)
- $a_{1805,SW} = 0.09\ g$ (soil class B)

These values produce permanent displacements (Figure 10), consistent with observed deformation/cracking without collapse dominance in the south sector.

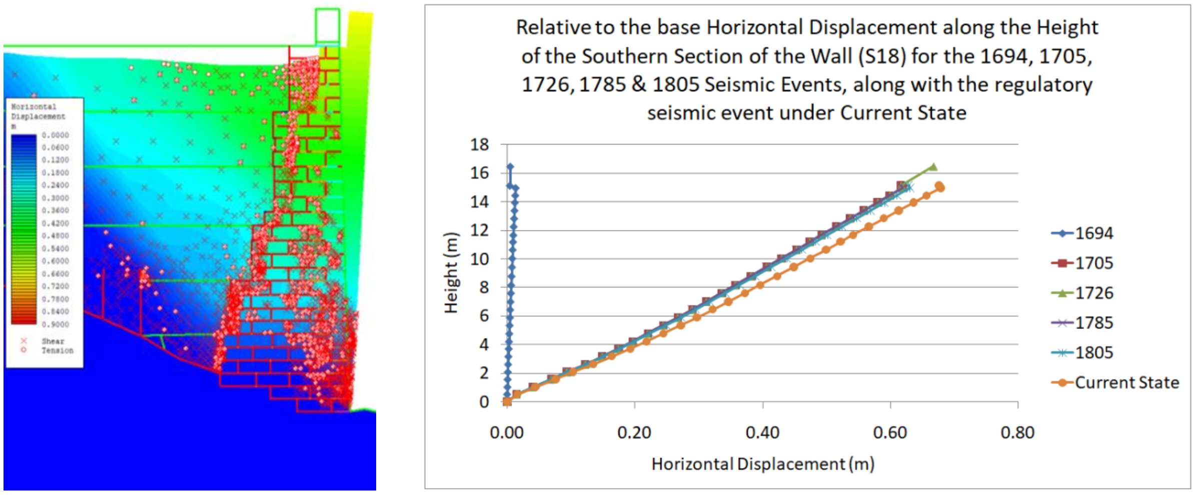

Figure 10. *Horizontal Displacement, yielded elements and areas of the South Wall in Area A6 (S18) under seismic load of* $\boldsymbol{a_{EW} = 0.13\,g}$ *that corresponds to the 1705 seismic event (Right). Relative to the base Horizontal Displacement along the height of the wall during the 1694, 1705, 1726, 1785 and 1805 seismic events along with the regulatory seismic event (*T_R*=1300) under Current State (Left).*

Northern CW cornice sector (SP1): progressive deterioration and collapse in 1805 (K1-defined)

Using $a_{eff.B} \approx 1.2 \cdot a_{eff,A}$, the north-sector NS (soil class A) effective accelerations consistent with the south staged calibration are:

- $a_{1705,SW} = \frac{0.13}{1.2} = 0.108\ g$ (soil class A)
- $a_{1805,SW} = \frac{0.09}{1.2} = 0.075\ g$ (soil class A)

The north cornice-sector collapse (Figure 11) is defined mechanically by K1 threshold crossing (δ/H) during the 1805 stage, interpreted as the decisive increment acting on a progressively weakened configuration.

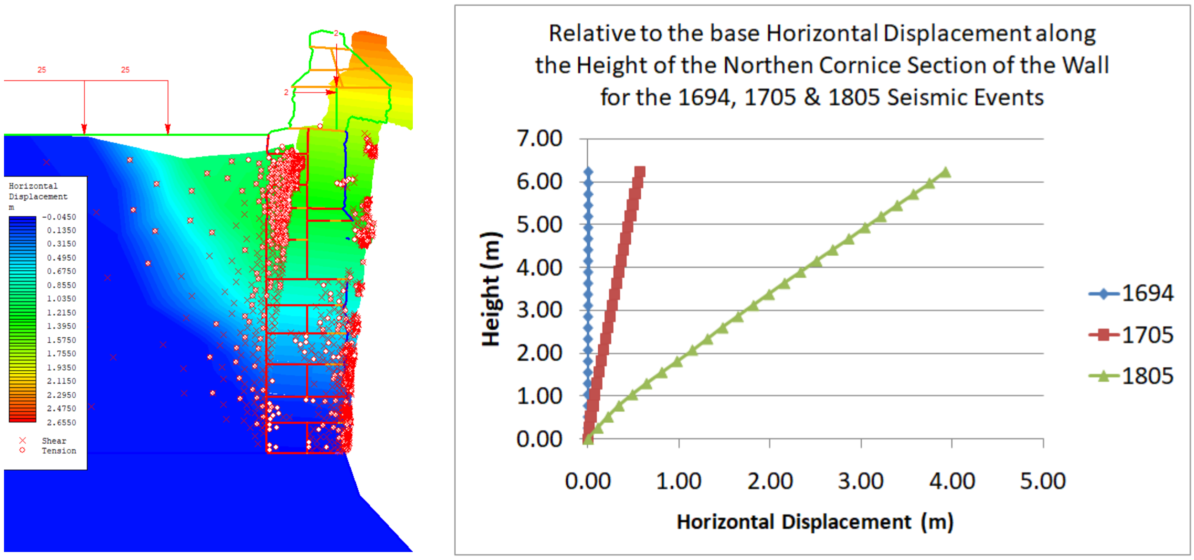

Figure 11. *Horizontal Displacement, yielded elements and areas of the North Wall near the cornice section under seismic load of* $\boldsymbol{a_{EW} = 0.108\ g}$ *that corresponds to the 1705 seismic event (Left). Horizontal Displacement along the height of the wall during the 1694, 1705 and 1805 seismic events (Right).*

CONCLUSIONS

This study presents a coherent forensic reconstruction of the seismic history recorded in the structural fabric of the Acropolis Circuit Wall (CW) and the adjacent Areopagus limestone detachment, demonstrating that these two independent mechanical archives can be reconciled within a unified geomechanical framework. By integrating architectural damage mapping, geomorphological characterization of joint-controlled rock failure, and seismological scenario constraints, a staged-history modelling strategy was developed that substantially reduces interpretive non-uniqueness and enables a physically grounded attribution of observed damage to specific historical earthquakes.

The principal methodological contribution lies in the formulation of a repeatable multidisciplinary workflow based on: (i) a structured evidence inventory (damage localization and chronology, mapped geological mechanisms, and macroseismic constraints), (ii) explicit definition of target mechanisms per sector of the wall and for the Areopagus detachment, (iii) adoption of a unified demand measure expressed in terms of peak ground acceleration (PGA) as a common intensity factor for both retaining-wall instability and joint sliding, (iv) staged-history SSI modelling that conditions later responses on prior damage and interventions, and (v) independent cross-checking through mechanically derived threshold accelerations. Within this framework, pseudostatic soil–structure interaction (SSI) analysis is employed not to reproduce transient response, but to evaluate permanent deformation and threshold states (including K1-defined collapse conditions), calibrated conceptually against dynamic SSI to justify the mapping between PGA and effective acceleration for comparable damage metrics.

The combined CW–Areopagus back-analyses support a consistent seismic narrative in which the 1705 earthquake generated an East–West demand level sufficient to (a) trigger collapse of the eastern CW sector, which acts as a collapse benchmark, and (b) reach the sliding threshold for the joint-controlled detachment at the Areopagus. The southern sector records cumulative deformation and cracking without global failure, consistent with repeated loading cycles that did not exceed its ultimate capacity. In contrast, the collapse of the northern cornice-bearing sector is interpreted as the outcome of progressive deterioration, with the 1805 earthquake constituting the decisive terminal event once the structure had been conditioned by earlier damage and mechanical degradation. Thus, the same event family produces sector-selective outcomes—collapse, permanent deformation, or delayed failure—depending on local resistance and mechanical history.

Quantitatively, the independently derived threshold accelerations for the Areopagus detachment and the eastern wall collapse are closely aligned. The modest discrepancy is consistent with the conservative modelling philosophy adopted for the CW, where characteristic (design-oriented) structural parameters were used, rendering the computed collapse acceleration a lower-bound estimate. This interpretation makes the direction of modelling bias explicit and avoids artificial forcing of exact numerical agreement. Furthermore, instrumental recordings from the 2019 NW Attica earthquake provide site-specific evidence of component asymmetry, with NS amplitudes typically 40–50% of EW for NW-source events, reinforcing the physical plausibility of the sector-selective damage pattern inferred for the 1705 and 1805 earthquakes.

From a broader seismotectonic perspective, the analyses indicate that the earthquakes of 1705 and 1805 were the decisive events affecting the CW and, more generally, the city of Athens, whereas subsequent earthquakes produced comparatively minor additional effects. The reconstructed demand levels are most consistent when anchored to macroseismic intensity-based estimates for these events, thereby providing engineering constraints that complement historical catalogues and regional seismic source models for the 18th–early 19th century period.

Finally, the proposed framework is transferable to other heritage contexts where structural damage and nearby geological failure mechanisms coexist as parallel seismic archives. The essential requirements are the ability to reconstruct a staged mechanical history, to define observable performance states linked to damage evidence, and to derive independent mechanical thresholds for cross-validation. In this sense, the Acropolis case study demonstrates how “seismic memory” embedded in stone can be decoded through integrated geomechanical analysis, transforming fragmentary historical damage into a quantitatively constrained narrative of past seismic demand.

ACKNOWLEDGEMENTS

The authors would like to express their sincere appreciation to Mr Manolis Tzannidakis, Civil Engineer (MSc), for his support in preparing the illustrative material and formatting the manuscript, as well as for his constructive comments and practical suggestions that improved clarity and presentation.

REFERENCES

Ambraseys, N.N. (1996), Material for the investigation of seismicity in Greece. Archaeo-Seismology (Eds S. Stiros and R.E.Jones). IGME and Br. Sch. Athens, Fitch Laboratory Occasional Paper, 7, 23-36.

CEN. (2004). Eurocode 8: Design of structures for earthquake resistance – Part 1: General rules, seismic actions and rules for buildings (EN 1998-1). Brussels: European Committee for Standardization.

CEN. (2005). *Eurocode 8: EN 1998-1:2004/A1:2005*. Brussels: European Committee for Standardization.

Egglezos, D., & Moullou, D. (2022). Documentation of strong earthquakes of the 18th century in connection with structural damage to the Circuit Wall of the Acropolis of Athens. In Proceedings of the 5th Hellenic Conference on Earthquake Engineering and Engineering Seismology.

Egglezos, D., Papadopoulos, C. Th., Papavasileiou, V., & Ioannidou, M. (2022). Permanent stabilization interventions to ensure the stability of the Acropolis of Athens perimeter wall Proceedings of the 6th Restoration Conference (ΕΤΕΠΑΜ).

Evgenikou, V. (2017). Geomatic and engineering analysis of large-scale rockfall at Areopagus Hill, Athens (Diploma thesis). National Technical University of Athens, School of Rural and Surveying Engineering.

GEO.PER. S.A. & DOMOS S.A. S.A. (2023). Geological and geotechnical investigation of the Acropolis rock mass and joint systems. Technical report, Athens, Greece.

Institute of Engineering Seismology & Earthquake Engineering (ITSAK). (2019). Strong motion records of the 19 July 2019 NW Attica earthquake (M5.1). Hellenic Strong Motion Network Database, Thessaloniki, Greece.

Koliopoulos, P.K., Margaris, B.N. & Klimis, N.S. (1998). Duration and energy characteristics of Greek strong motion records. Journal of Earthquake Engineering, 2(3), 391–417.

Korres M. (1996), Seismic damage to the monuments of the Athenian Acropolis. Archaeo-Seismology (Eds S. Stiros and R.E.Jones). IGME and Br. Sch. Athens, Fitch Laboratory Occasional Paper, 7, 69-74

Mylonakis, G., & Gazetas, G. (2000). Seismic soil–structure interaction: Beneficial or detrimental? Journal of Earthquake Engineering, 4(3), 277–301.

Papazachos, B. C., & Papazachou, C. (2003). The earthquakes of Greece. Thessaloniki: Ziti Publications.

Rinaldis, D., Berardi, R., Theodulidis, N.P. & Margaris, B.N. (1998). Empirical predictive models based on a joint Italian and Greek strong motion database: I. Peak ground acceleration and velocity. In Proceedings of the 11th European Conference on Earthquake Engineering (CD-ROM), Paris.

Skarlatoudis, A. A., Papazachos, C. B., Margaris, B. N., & Theodulidis, N. P. (2003). Empirical peak ground-motion predictive relations for shallow earthquakes in Greece. Bulletin of the Seismological Society of America, 93(6), 2591–2603.

YSMA Technical Office for the Walls. (2020). Strategic Intervention Plan for the Walls of the Acropolis of Athens. YSMA Archive.